16th World Conference on Earthquake, 16WCEE 2017

Santiago Chile, January 9th to 13th 2017

Paper N° 701 (Abstract ID)

Registration Code: S-V1460455203

CROSS EVOLUTIONARY POWER SPECTRA ESTIMATION OF SPATIALLY VARIABLE SEISMIC GROUND MOTIONS VIA HARMONIC WAVELETS

D. Wang(1), ZL. Fan(2)

(1) *Lecturer, School of Civil Engineering & Mechanics, Yanshan University, wangding@ysu.edu.cn*
(2) *M. S. Candidate, School of Civil Engineering & Mechanics, Yanshan University, fanzenglei1011@163.com*

Abstract

Nonstationary characteristics of spatially variable seismic ground motions, which are mathematically described by cross evolutionary power spectra or evolutionary coherency, have significant effect on earthquake responses of nonlinear extended structures. Estimation and modeling of cross evolutionary power spectral density (EPSD) of spatially variable seismic ground motions are of interest in recent years for engineering purposes. This article presents an approach for estimating the cross EPSD of the spatially variable seismic ground motions by using the generalized harmonic wavelets (GHW). The cross EPSD and the evolutionary lagged coherency of the realistic spatially variable seismic ground motions are estimated by this approach. The time-varying nonstationary characteristics of these ground motions are also analyzed. First, after a brief review of the former studies in wavelets-based evolutionary spectra estimation, a cross EPSD estimation formula is derived using the GHW within the framework of evolutionary spectra estimation given by Spanos & Failla. Then, the proposed estimation formula is used to estimate the cross EPSDs of the seismic ground motions recorded at the SMART-1 array during Event 45. The cross EPSDs and the evolutionary lagged coherency between the center station and the outer ring stations, at separation distances of 2000m, are obtained. The comparisons of the estimated lagged coherency at different times indicate that the correlation of the spatially variable seismic ground motions is time-dependent. During the stable stage of the ground-motion intensity, the lagged coherency is close to 0.8 in the low frequency range and decays as frequency increasing. During the rising and decaying stages of the ground-motion intensity, the lagged coherency is fluctuant with a mean value of about 0.4.

Keywords: cross evolutionary power spectral density, evolutionary lagged coherency, seismic ground motion, generalized harmonic wavelets

1. Introduction

For long-span structural analysis and design, it is necessary to consider the spatial variation of seismic ground motions. Usually, the earthquake ground motion field on the engineering site surface is treated as a stationary, homogenous and isotropy random field. The models of power spectral density, cross spectral density and lagged coherency are used to describe the auto- and cross-correlation properties of the ground motion random field [1]. However, numerous studies have shown that the nonstationary characteristics of seismic ground motions have significant effect on the responses of nonlinear structures and cannot be ignored, which requires that the seismic ground motion field should be modeled as nonstationary random field [2, 3].

As proposed by Priestley, evolutionary power spectral density (EPSD) and cross evolutionary power spectral density are powerful tools to describe the nonstationarity of stochastic process or random field [4]. So far, several methods have been presented to estimate the EPSD of nonstationary stochastic process, including the wavelets-based method. Due to the time localization properties of wavelet basis, it is possible to use wavelets to identify the temporal variation of the spectral characteristics of nonstationary stochastic process. A general method for evolutionary spectra estimation using wavelets was proposed by Spanos & Failla [5], and has been improved for cross evolutionary spectra estimation by Huang & Chen [6]. Spanos *et al* used the harmonic wavelets (HW) and the generalized harmonic wavelets (GHW), which are both proposed by Newland [7, 8], to estimate the evolutionary spectra of stochastic processes [9]. The results showed that the HW and the GHW are effective tools for the evolutionary spectrum estimation because their spectra are nonoverlapping in the frequency domain.

In this paper, the GHW is applied to estimate the cross EPSD and evolutionary lagged coherency of random field. The cross EPSD and the evolutionary lagged coherency of the realistic seismic ground motions recorded by the SMART-1 array, Taiwan, are estimated by using this GHW-based method. The time-varying characteristics of the evolutionary lagged coherency are presented and analyzed.

2. Cross evolutionary power spectra estimation via GHW

Two real-valued processes, $f_1(t)$ and $f_2(t)$, as defined by Priestley [4], can be expressed as

$$\begin{aligned} f_1(t) &= \int_{-\infty}^{+\infty} A_1(\omega,t)\cdot e^{i\omega t}\cdot \mathrm{d}\bar{Z}_1(\omega) \\ f_2(t) &= \int_{-\infty}^{+\infty} A_2(\omega,t)\cdot e^{i\omega t}\cdot \mathrm{d}\bar{Z}_2(\omega) \end{aligned} \tag{1}$$

in which $A_1(\omega,t)$, $A_2(\omega,t)$ are amplitude envelope functions and $\mathrm{d}\bar{Z}_1(\omega)$, $\mathrm{d}\bar{Z}_2(\omega)$ are complex-valued zero-mean orthogonal increment random processes. The cross EPSD of $f_1(t)$ and $f_2(t)$ is given as [10]

$$S_{f_1 f_2}(\omega) = A_1(\omega,t)\cdot A_2^*(\omega,t)\cdot S_{\bar{f}_1\bar{f}_2}(\omega) \tag{2}$$

in which $S_{\bar{f}_1\bar{f}_2}(\omega)$ is the cross power spectral density of the stationary processes corresponding to Eq. (1), as

$$\begin{aligned} \bar{f}_1(t) &= \int_{-\infty}^{+\infty} e^{i\omega t}\cdot \mathrm{d}\bar{Z}_1(\omega) \\ \bar{f}_2(t) &= \int_{-\infty}^{+\infty} e^{i\omega t}\cdot \mathrm{d}\bar{Z}_2(\omega) \end{aligned} \tag{3}$$

The cross EPSD, $S_{f_1 f_2}(\omega)$, can be estimated by wavelets. In this paper, the generalized harmonic wavelet (GHW) is used to estimating the cross EPSD. As defined by Newland [8], the GHW of level *m*, *n* is expressed as

$$w_{m,n}\left(t-\frac{k}{n-m}\right) = \frac{\exp\{2\pi n i(t-\frac{k}{n-m})\} - \exp\{2\pi m i(t-\frac{k}{n-m})\}}{2\pi i(n-m)(t-\frac{k}{n-m})} \tag{4}$$

in which *k* must be an integer. The Fourier transform of Eq. (4) is

$$W_{m,n}(\omega)=\begin{cases}\dfrac{1}{2\pi(n-m)}\exp\{-i\omega k/(n-m)\}, & 2\pi m\le\omega<2\pi n\\ 0, & \text{elsewhere}\end{cases}\tag{5}$$

Fig. 1 presents the Fourier amplitude spectrum of the GHW of level *m*, *n*. In the frequency domain, the amplitude spectrum of the GHW is a constent during the interval $[2\pi m,\ 2\pi n)$ and is zero elsewhere.

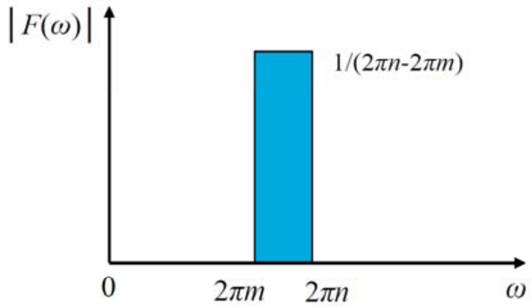

Fig. 1 – Fourier amplitude spectrum of the GHW of level *m*, *n*

For a real-valued time process $f(t)$, the GHW coefficients are defined as

$$c_{m,n,k}=(n-m)\cdot\int_{-\infty}^{+\infty}f(t)\cdot w_{m,n}^{*}(t-\frac{k}{n-m})\mathrm{d}t\tag{6}$$

$f(t)$ can be reconstructed by the GHW coefficients as

$$f(t)=2\,\mathrm{Re}\sum_{m,n}\sum_{k=-\infty}^{+\infty}c_{m,n,k}\cdot w_{m,n}(t-\frac{k}{n-m})\tag{7}$$

Taking Eq. (1) into Eq. (6),

$$\begin{aligned}c_{m,n,k}^{1}&=(n-m)\int_{-\infty}^{+\infty}\{\int_{-\infty}^{+\infty}A_1(\omega,t)\cdot e^{i\omega t}\cdot\mathrm{d}\bar{Z}_1(\omega)\}\cdot w_{m,n}^{*}(t-\frac{k}{n-m})\mathrm{d}t\\&=(n-m)\int_{-\infty}^{+\infty}\{\int_{-\infty}^{+\infty}A_1(\omega,t)\cdot e^{i\omega t}\cdot w_{m,n}^{*}(t-\frac{k}{n-m})\cdot\mathrm{d}t\}\cdot\mathrm{d}\bar{Z}_1(\omega)\end{aligned}\tag{8}$$

Due to the time localization properties of the GHW at the vicinity of $k/(n-m)$, it is reasonable to assume that $A_1(\omega,t)$ changes much more slowly than $w_{m,n}^{*}(t-k/(n-m))$, and Eq. (8) can be represented as

$$c_{m,n,k}^{1}=(n-m)\int_{-\infty}^{+\infty}A_1(\omega,\frac{k}{n-m})\cdot\{\int_{-\infty}^{+\infty}e^{i\omega t}\cdot w_{m,n}^{*}(t-\frac{k}{n-m})\cdot\mathrm{d}t\}\cdot\mathrm{d}\bar{Z}_1(\omega)\tag{9}$$

Defining $\tau=t-k/(n-m)$, $\mathrm{d}\tau=\mathrm{d}t$, Eq. (9) is rewritten as

$$\begin{aligned}c_{m,n,k}^{1}&\approx(n-m)\int_{-\infty}^{+\infty}\{\int_{-\infty}^{+\infty}w^{*}(\tau)\cdot e^{i\omega\tau}\mathrm{d}\tau\}\cdot A_1(\omega,\frac{k}{n-m})\cdot e^{\frac{i\omega k}{n-m}}\cdot\mathrm{d}\bar{Z}_1(\omega)\\&=(n-m)\int_{-\infty}^{+\infty}2\pi\cdot W_{m,n}^{*}(\omega)\cdot A_1(\omega,\frac{k}{n-m})\cdot e^{\frac{i\omega k}{n-m}}\cdot\mathrm{d}\bar{Z}_1(\omega)\\&=\int_{-\infty}^{+\infty}A_1(\omega,\frac{k}{n-m})\cdot e^{\frac{i\omega k}{n-m}}\cdot\mathrm{d}\bar{Z}_1{}'(\omega)\end{aligned}\tag{10}$$

in which

$$\mathrm{d}\bar{Z}_1{}'(\omega)=2\pi(n-m)\cdot W_{m,n}^{*}(\omega)\cdot\mathrm{d}\bar{Z}_1(\omega)\tag{11}$$

Eq. (10) indicates that the GHW coefficient, $c_{m,n,k}^{1}$, is a nonstationary process with respect to the discrete time translation parameter $k/(n-m)$. Similarly,

$$c_{m,n,k}^{2}=\int_{-\infty}^{+\infty}A_{2}(\omega,\frac{k}{n-m})\cdot e^{\frac{i\omega k}{n-m}}\cdot \mathrm{d}\bar{Z}_{2}'(\omega) \tag{12}$$

in which

$$\mathrm{d}\bar{Z}_{2}'(\omega)=2\pi(n-m)\cdot W_{m,n}^{*}(\omega)\cdot \mathrm{d}\bar{Z}_{2}(\omega) \tag{13}$$

According to Eq. (2), the cross EPSDs of $c_{m,n,k}^{1}$ and $c_{m,n,k}^{2}$ is

$$\begin{aligned}S_{c^1c^2}^{m,n}(\omega,\frac{k}{n-m})&=4\pi^2(n-m)^2\cdot A_1(\omega,\frac{k}{n-m})\cdot A_2^{*}(\omega,\frac{k}{n-m})\cdot\left|W_{m,n}(\omega)\right|^2\cdot S_{\bar{f}_1\bar{f}_2}(\omega)\\&=4\pi^2(n-m)^2\cdot\left|W_{m,n}(\omega)\right|^2\cdot S_{f_1f_2}(\omega,\frac{k}{n-m})\end{aligned} \tag{14}$$

The instantaneous cross covariance of $c_{m,n,k}^{1}$ and $c_{m,n,k}^{2}$ can be calculated by $S_{c^1c^2}^{m,n}(\omega,\frac{k}{n-m})$, as

$$\begin{aligned}E[c_{m,n,k}^{1}\cdot c_{m,n,k}^{2}{}^{*}]&=\int_{-\infty}^{+\infty}S_{c^1c^2}^{m,n}(\omega,\frac{k}{n-m})\cdot \mathrm{d}\omega\\&=4\pi^2(n-m)^2\cdot\int_{-\infty}^{+\infty}\left|W_{m,n}(\omega)\right|^2\cdot S_{f_1f_2}(\omega,\frac{k}{n-m})\cdot \mathrm{d}\omega\end{aligned} \tag{15}$$

Taking Eq. (5) into Eq. (15),

$$\frac{E[c_{m,n,k}^{1}\cdot c_{m,n,k}^{2}{}^{*}]}{2\pi(n-m)}=\frac{\int_{2m\pi}^{2n\pi}S_{f_1f_2}(\omega,\frac{k}{n-m})\cdot \mathrm{d}\omega}{2\pi(n-m)} \tag{16}$$

The right side of Eq. (16) is the mean value of $S_{f_1f_2}(\omega,t)$ during the frequency-domain interval $\left[m,n\right)$ at the time $t=k/(n-m)$. Here, we use the mean value of $S_{f_1f_2}(\omega,t)$ as the estimated unsmoothed cross EPSD, $\hat{S}_{f_1f_2}(\omega,t)$, as

$$\hat{S}_{f_1f_2}(\omega,t)=\frac{\int_{2m\pi}^{2n\pi}S_{f_1f_2}(\omega,t)\cdot \mathrm{d}\omega}{2\pi(n-m)} \tag{17}$$

From Eq. (16), the cross EPSD of $f_1(t)$ and $f_2(t)$ can be estimated by the GHW coefficients, as

$$\hat{S}_{f_1f_2}(\omega,t)=\frac{E[c_{m,n,k}^{1}\cdot c_{m,n,k}^{2}{}^{*}]}{2\pi(n-m)} \tag{18}$$

In this paper, the GHWs with the same bandwidth Δ are used, which means the bandwidth $\Delta=n-m$ is a constant for different level *m*, *n*, and Eq. (18) can be rewritten as

$$\hat{S}_{f_1f_2}(\omega,t)=\frac{E[c_{m,n,k}^{1}\cdot c_{m,n,k}^{2}{}^{*}]}{2\pi\Delta} \tag{19}$$

It should be noted that Eq. (19) is available to estimated the auto EPSD of a time process $f(t)$ by making $f_1(t)=f(t)$ and $f_2(t)=f(t)$, as

$$\hat{S}_{ff}(\omega,t)=\frac{E[\left|c_{m,n,k}\right|^2]}{2\pi\Delta} \tag{20}$$

Eq. (19) and (20) can be used to estimate the evolutionary spectra of the realistic spatially variable seismic ground motion records. Fig. 2 presents the E-W components of the ground motion time histories recorded at stations C00 and O01 at the SMART-1 array, Taiwan, during Event 45 in 1986. Station C00 is at the center of the array and station O01 is on the outer ring. For the outer ring, the radius is 2000 m. The sampling intervals of these two ground motion records are both 0.01s.

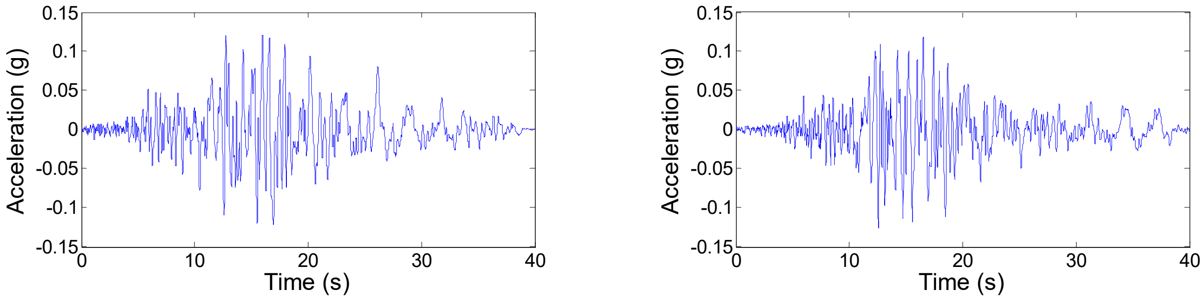

(a) (b)

Fig. 2 – Time histories recoreded at stations (a) C00 and (b) O01 at the SMART-1 array during Event 45 in the E-W direction.

Fig. 3 shows the estimated EPSDs of the ground motions in Fig. 2 by using Eq. (20). The frequency-domain bandwidth Δ is 1 Hz and the time-domain interval $1/(n-m)$ is 1 sec. The estimated EPSDs indicate that the energy of the ground motion at C00 distributes more concentratedly than that of the ground motion at O01. Fig. 4 presents the real and imaginary parts of the unsmoothed cross EPSD of these ground motions estimated by Eq. (19).

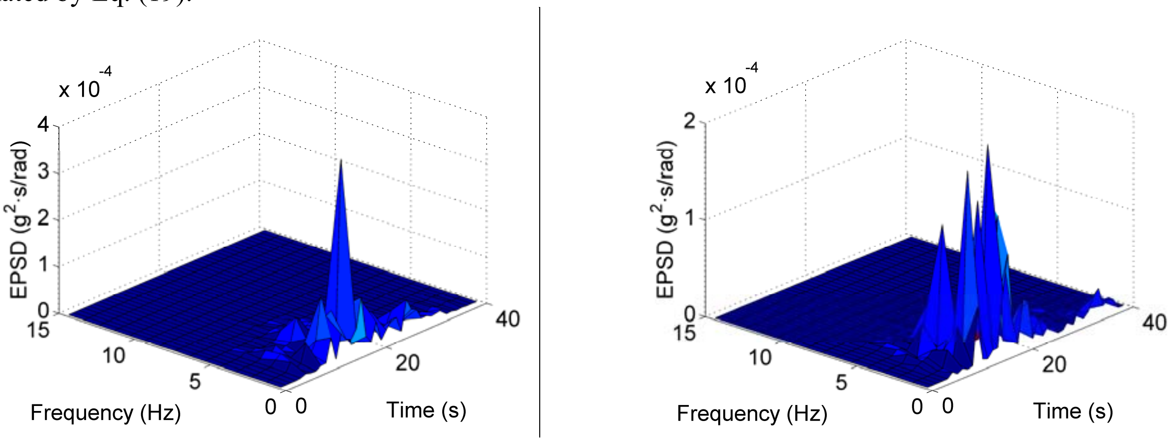

(a) (b)

Fig. 3 – Unsmoothed EPSDs of the seismic ground motions at (a) C00 and (b) O01 shown in Fig. 1.

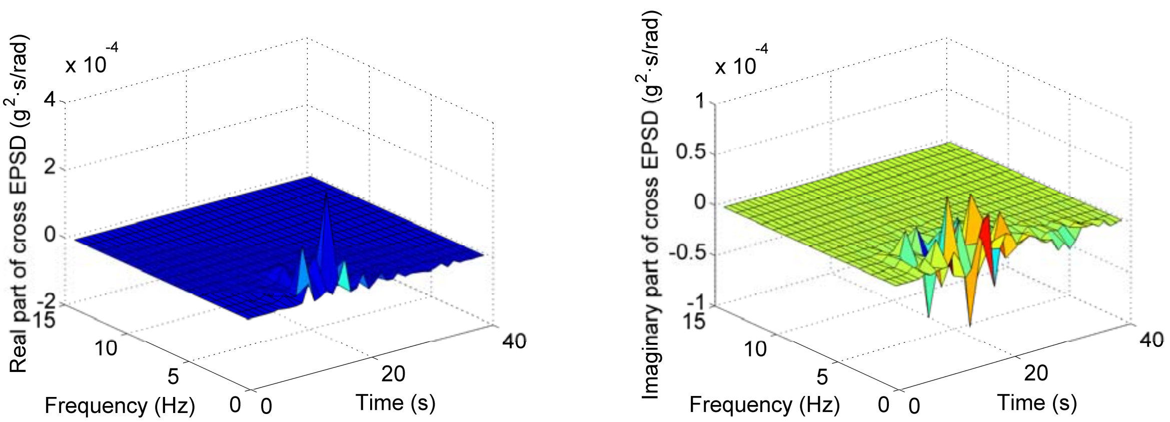

(a) (b)

Fig. 4 – (a) Real and (b) imaginary parts of the unsmoothed cross EPSD of the seismic ground motions in Fig. 2.

3. Evolutionary lagged coherency of spatially variable ground motions

In earthquake engineering, lagged coherency is usually used to describe the correlation of spatially variable seismic ground motions instead of cross spectrum. For two nonstationary processes $f_1(t)$ and $f_2(t)$, the evolutionary lagged coherency is defined as

$$\left|\bar{\gamma}^M_{f_1 f_2}(\omega,t)\right| = \frac{\left|\bar{S}^M_{f_1 f_2}(\omega,t)\right|}{\sqrt{\bar{S}^M_{f_1 f_1}(\omega,t)\cdot \bar{S}^M_{f_2 f_2}(\omega,t)}} \tag{21}$$

in which $\bar{S}^M_{f_1 f_1}(\omega,t)$, $\bar{S}^M_{f_2 f_2}(\omega,t)$ and $\bar{S}^M_{f_1 f_2}(\omega,t)$ are the smoothed evolutionary spectra corresponding to the estimated unsmoothed spectra $\hat{S}_{f_1 f_1}(\omega,t)$, $\hat{S}_{f_2 f_2}(\omega,t)$ and $\hat{S}_{f_1 f_2}(\omega,t)$. The estimated evolutionary spectra can be smoothed by using the M-point Hamming windows.

The cross EPSDs of the seismic ground motions at the center station C00 and at the outer-ring stations during event 45 are estimated and smoothed for the evolutionary lagged coherency calculation. The outer-ring stations include O01, O02, O04, O06, O07, O08, O10 and O12. The 3-point Hamming windows are used to smooth the estimated cross EPSDs. The evolutionary lagged coherency is calculated by Eq. (21). Figs. 5 ~ 7 present the average lagged coherency curves at different time. The lagged coherency curves of the center and the outer-ring stations are shown as dotted lines and the average lagged coherency curves are shown as blue solid lines.

From 2 to 8 sec, as shown in Fig. 5, the average lagged coherency curves fluctuate with a mean value about 0.4. The decreasing tendency of the lagged coherency with increasing frequency is not remarkable. Most of the mean values of the lagged coherency are less than 0.6.

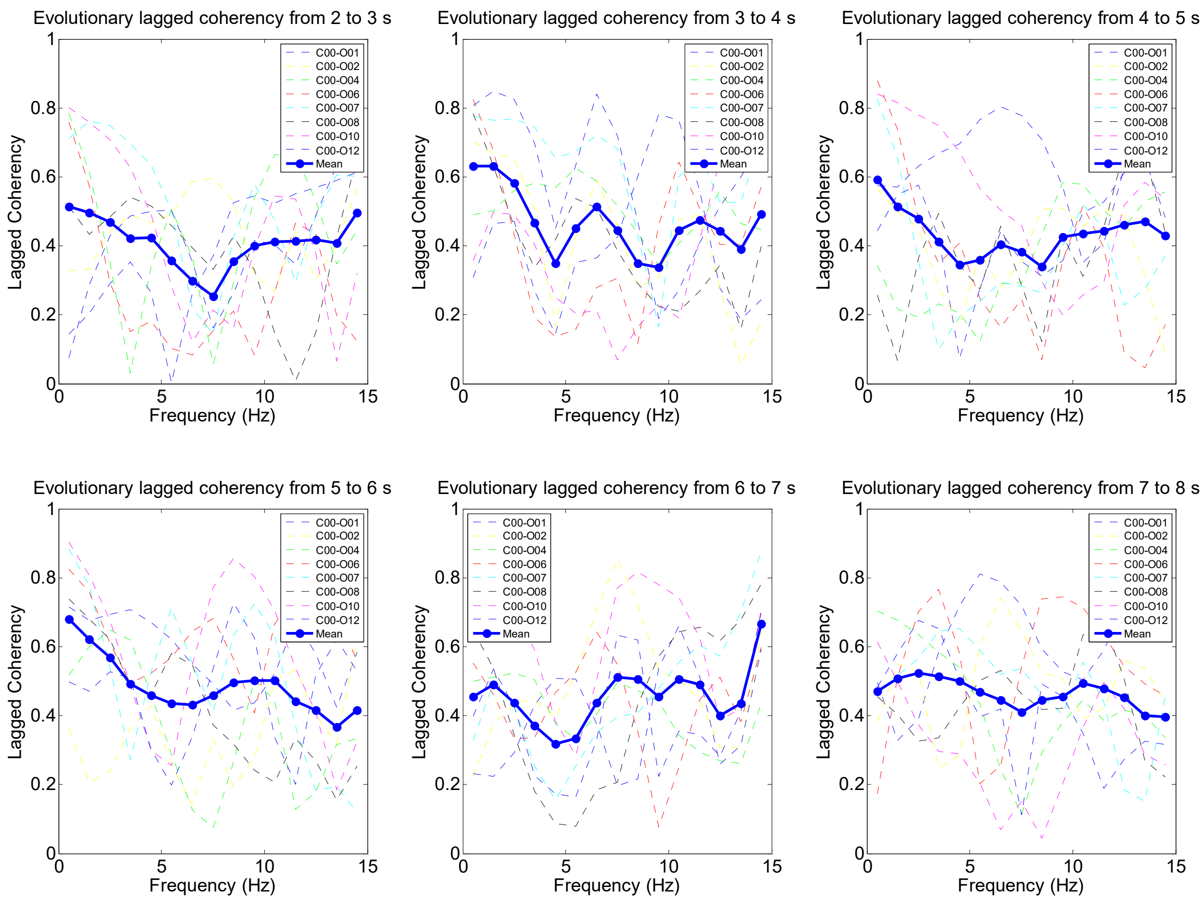

Fig. 5 – Evolutionary lagged coherency from 2 to 8 sec.

The average lagged coherency from 8 to 17 sec is quite different from these from 2 to 8 sec. From 8 to 17 sec, the mean values of the lagged coherency nearby 0 Hz reach 0.8. The lagged coherency is gradually decreasing to 0.4 with increasing frequency in the range of 0-5 Hz and then keeps stable.

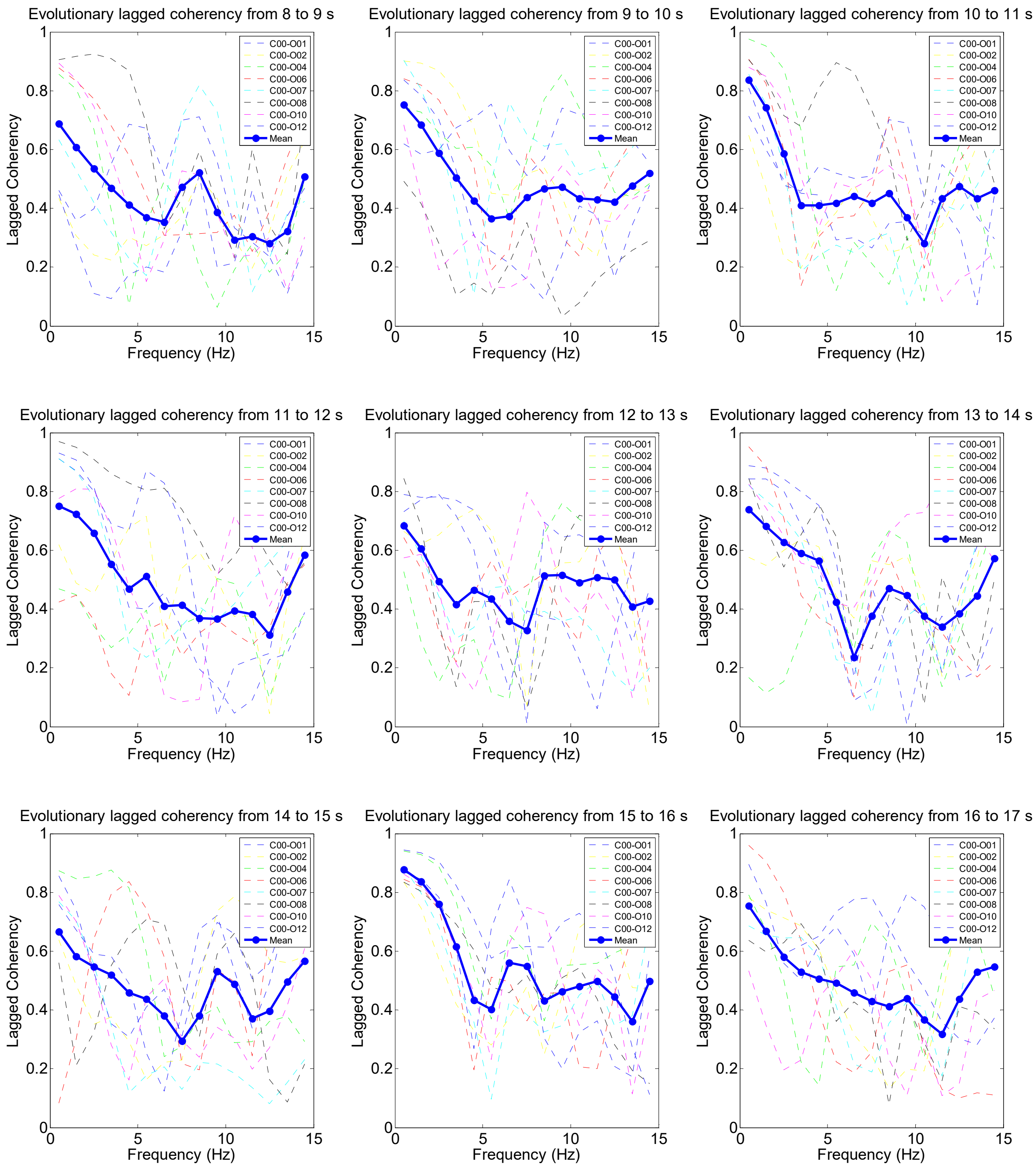

Fig. 6 – Evolutionary lagged coherency from 8 to 17 sec.

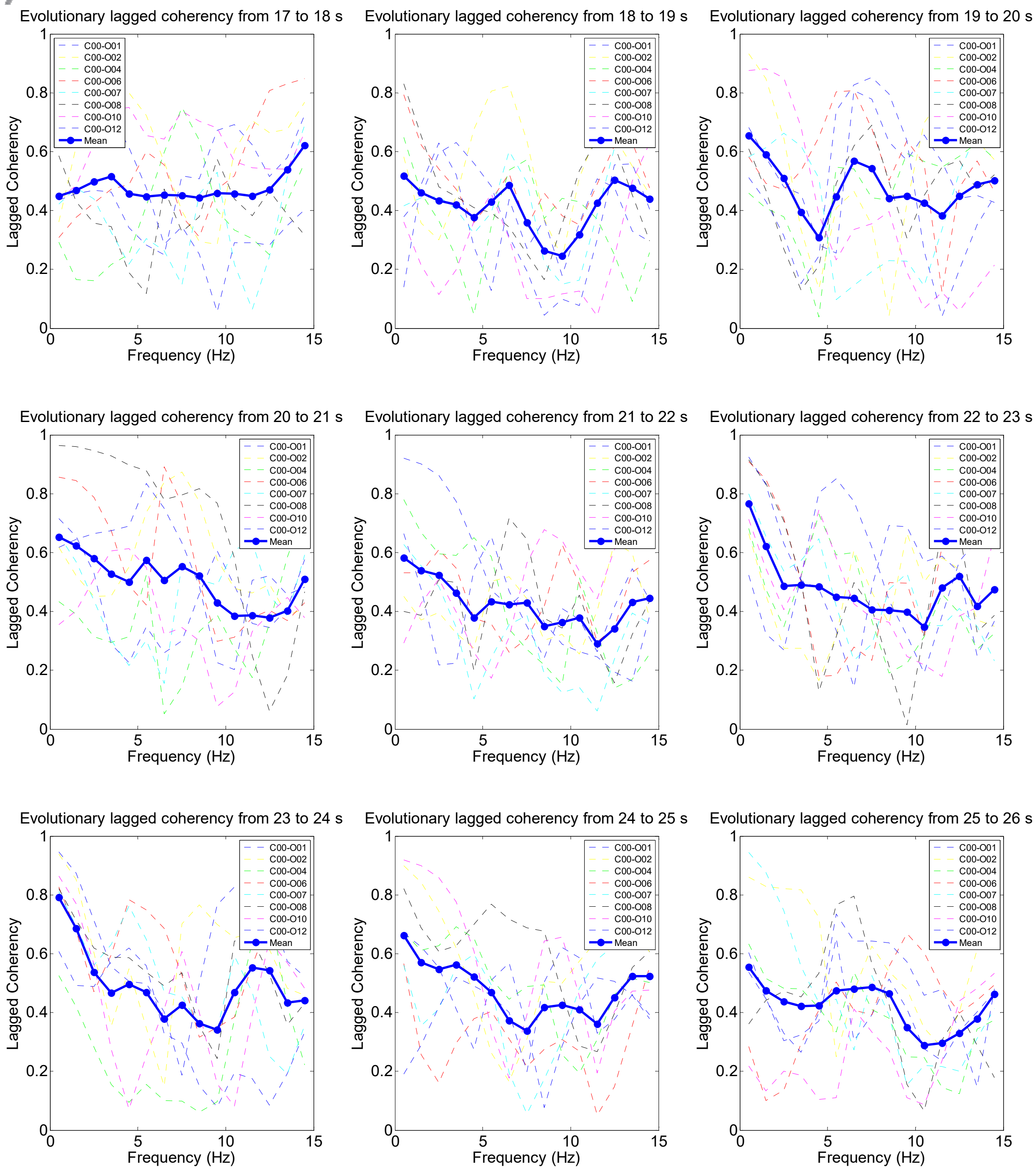

Fig. 7 – Evolutionary lagged coherency from 17 to 26 sec.

From 17 to 26 sec, the characteristics of the average lagged coherency curves are complex. The decreasing tendency of the lagged coherency with increasing frequency is not as obvious as that from 8 to 17 sec and the mean values are mostly less than 0.6. However, from 22 to 24 sec, the lagged coherency in the low frequency range is high and close to 0.8 when the frequency trends to 0 Hz.

4. Analysis

As shown above, the characteristics of the evolutionary lagged coherency changes with time, which means that the cross correlation of the spatilly variable seismic ground motions are nonstationary. Generally, according to the intensity variation, a seismic ground motion process can be divided into three stages [11, 12]. In the beginning, the seismic ground motion starts and its intensity is increasing. Then, the intensity of the seismic ground motion tends to be stable for a few seconds or minutes. After that, the ground motion is gradually decaying. The cumulative enery curve of the seismic ground motion can show these three stages clearly. The cumulative energy curve of a process $f(t)$ is defined as

$$\int_0^t f^2(\tau)\cdot \mathrm{d}\tau \tag{22}$$

In Fig. 8, the blue line is the mean cumulative energy curve of the seismic ground motions which are used to estimate the evolutionary lagged coherency shown in Figs. 5 ~7. From 4 to 11 sec, the slope of the mean cumulative energy curve increases, which means the intensity of the seismic ground motion becomes larger gradully. Then, from 11 to 20 sec, the mean cumulative energy curve changes linearly and the seismic ground motion comes into the indensity-stable stage. After 20 sec, the slope of the mean cumulative energy curve becomes small again,which indicates that the seismic ground motion intensity is decaying.

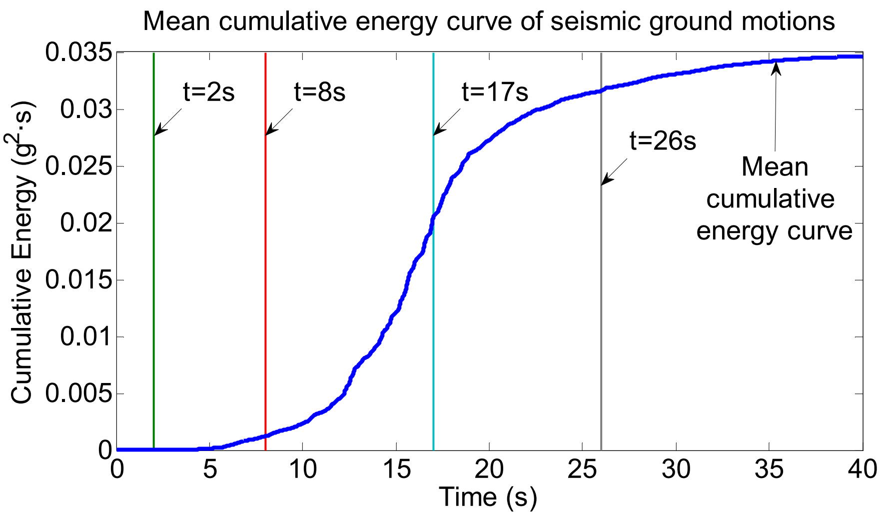

Fig. 8 – Mean cumulative energy curve of the seismic ground motions.

The time points at which the characteristics of the evolutionary lagged coherency changes are still marked out in Fig. 8. It can be seen that, though the variation of the lagged coherency occurs about 2 sencods earlier than that of the ground motion intensity, the time segments in which the evolutionary lagged coherency presents different characteristics are consistent with the intensity-increasing, -stable and -decaying stages of the seismic ground motions. A possible reason for this phenomenon is that different types of earthquake waves, such as P wave, S wave and surface waves, arrive at the station array with time delays. The correlation and the intensity of each type of earthquake wave are different from those of others, which causes that the correlation variation of the seismic ground motions are consistent with the intensity variation.

5. Conclusions

This study presents a GHW-based method for estimating the cross EPSDs of nonstationary stochastic processes. Applying this approach, the cross EPSDs and the evolutionary lagged coherency of the spatially variable seismic ground motions at the SMART-1 array during Event 45 are obtained. The estimation results indicate that the correlation of these ground motion records changes with time significantly. The nonstationarity of the spatially variable seismic ground motions is remarkable.

The derivation of the cross EPSD estimation formula is within the framework of evolutionary spectra estimation proposed by Spanos & Failla. In this paper, the GHWs are used for the cross EPSD estimation. Because the spectra of the GHWs are nonoverlapping in the frequency domain, the cross EPSD can be represented in an explcit form of the GHW coefficients instead of by solving integral equations for the genaral situation, which makes the cross spectra estimation formula simple and convenient for application.

The cross EPSDs of the seismic ground motions between the center station and the outer-ring stations at the SMART-1 array during Event 45 are estimated by using the proposed GHW-based method. The evolutionary lagged coherency is calculated by using the estimated cross EPSDs and exhibits a significant change with time. The evolutionary process of the lagged coherency can be divided into three stages. During the first and third stages, corresponding to the rising and decaying stages of the earthquake ground motion intensity, the lagged coherency is mostly less than 0.6 and fluctuant with a mean value of about 0.4. During the second stage, corresponding to the stable stage of the earthquake ground motion intensity, the lagged coherency is close to 0.8 in the low frequency range and decreases as frequency increasing.

An apparent limitation of this study is that the spatially variable seismic ground motion records are just from one earthquake event. More earthquake events will be investigated in further research. Additional work is warranted for the determination of the parametric model of the cross EPSD or the evolutionary coherency.

6. Acknowledgments

This research was supported by the National Natural Science Foundation of China (Grant No. 51408526) and Natural Science Foundation of Hebei Province (E2015203274).

7. References

[1] Zerva A (2009): *Spatial Variation of Seismic Ground Motions: Modeling and Engineering Applications*. CRC Press.

[2] Yeh CH, Wen YK (2002). Modeling of non-stationary ground motion and analysis of inelastic structural response. *Structural Safety*, **8**, 281-298.

[3] Wang J, Fan L, Qian S, Zhou J (2002). Simulations of non-stationary frequency content and its importance to seismic assessment of structures. *Earthquake Engineering and Structural Dynamics*, **31**: 953-1005.

[4] Priestley MB (1965). Evolutionary spectra and nonstationary processes. *Journal of the Royal Statistical Society*, *Series A*, **27**: 204-237.

[5] Spanos PD, Failla G (2004). Evolutionary spectra estimation using wavelets. *Journal of Engineering Mechanics*, *ASCE*, **130**: 952-960.

[6] Huang GQ, Chen XZ (2009). Wavelets-based estimation of multivariate evolutionary spectra and its application to nonstationary downburst winds. *Engineering Structures*, **31**: 976-989.

[7] Newland DE (1993). Harmonic wavelet analysis. *Proceedings of the Royal Society A: Mathematical, Physical and Engineering Science*, **443**: 203-205

[8] Newland DE (1994). Harmonic and Music Wavelets. *Proceedings of the Royal Society A: Mathematical, Physical and Engineering Science*, **444**: 605-620

[9] Spanos PD, Tezcan J, Tratskas P (2005). Stochastic processes evolutionary spectrum estimation via harmonic wavelets. *Computer Methods in Applied Mechanics and Engineering*, **194**: 1367-1383.

[10] Michaelov G, Sarkani S, Lutes LD (1999). Spectral characteristics of nonstationary random processes — a critical review. *Structural Safety*, **21**: 223-244

[11] Jennings PC, Housner GW, Tsai NC (1968): Simulated earthquake motions. *Technical Report*, Earthquake Engineering Research Laboratory, California Institute of Technology, Pasadena, California, USA.

[12] Amin M, Ang A H-S (1968). Non-stationary stochastic models of earthquake motion. *Journal of Engineering Mechanics Division*, *ASCE*, **94**: 559- 583